Time-Resolved Ballistic Acceleration of Electrons in a GaAs Quantum-Well Structure

W. Sha[a] and T. B. Norris
Ultrafast Science Laboratory, University of Michigan, 2200 Bonisteel, Ann Arbor, Michigan 48109-2099

W. J. Schaff
School of Electrical Engineering, Cornell University, Ithaca, New York 14850

K. E. Meyer
Cavendish Laboratory, Cambridge University, Cambridge, CB3 0HE, United Kingdom
(Received 8 July 1991)

We have used femtosecond time-resolved optical-absorption spectroscopy to study the dynamics of high-field parallel transport of electrons in GaAs quantum wells. We have directly observed the ballistic acceleration of electrons from the band edge by measuring the nonequilibrium transient energy distribution of the electrons. The ballistic acceleration occurs on a 150-fs time scale.

PACS numbers: 72.20.−i, 72.40.+w, 78.30.−j

If an electron moves through a crystal without scattering, its transport is termed ballistic. One way to observe ballistic effects in transport is to monitor the electron transport over a distance short compared to the mean free path. Recent advances in nanofabrication technology have enabled devices of the required small dimensions to be produced, and this has given rise to a substantial body of work on effects of ballistic drift on transport in various structures [1–3]. One example of such a structure is the heterojunction bipolar transistor, in which the base is of submicron length. Electrons are launched across a heterojunction into the field-free base region with a certain excess energy E_e above the band edge. Some fraction of the electrons are found to drift ballistically across the base.

A complementary approach to the use of nanostructures to observe ballistic transport is to time resolve the transport on a time scale shorter than the mean scattering time. This scattering time is of the order of 100 fs, which is a time scale accessible by techniques of femtosecond optical spectroscopy [4,5]. In this Letter we describe the observation of ballistic acceleration of electrons in the presence of a strong electric field, by injecting carriers at the band edge and monitoring the time-dependent distribution function of the electrons directly via the changes in the optical absorption spectrum. We believe this experiment is significant in two respects. First, it extends standard pump-probe techniques to the study of transient carrier distributions in the presence of a strong electric field. Second, though time-averaged ballistic *drift* of electrons has been extensively studied, to the authors' knowledge there has up to now been no time-resolved observation of ballistic *acceleration* in an external electric field.

The basic scheme of the experiment is to photoinject electron-hole pairs with a short (100 fs) optical pulse into a GaAs multiple-quantum-well (MQW) structure, where a strong electric field is applied *in the plane* of the quantum wells. The pump laser is in fact tuned to resonantly generate electron–heavy-hole excitons, so the carriers have initially no kinetic energy. (It is essential to start with a cold distribution so that the measurement is sensitive only to heating effects at early times.) As the carriers accelerate and gain energy from the field, a broadband 100-fs pulse probes the change in the optical absorption due to the changes in the carrier distributions f. The time resolution of the experiment is comparable to the principal relevant scattering processes, namely, carrier-carrier and carrier–LO-phonon scattering, allowing the observation of ballistic effects in the transport. At the highest electric field studied (nominally 16 kV/cm), we have observed evidence of ballistic acceleration of electrons on a 150-fs time scale.

The sample for this experiment consisted of a 40-period undoped (50-Å GaAs)/(150-Å $Al_{0.3}Ga_{0.7}As$) MQW structure grown by molecular-beam epitaxy. The sample was capped by a 500-Å i-$Al_{0.3}Ga_{0.7}As$ layer and a 1000-Å n^+-GaAs layer, on which was fabricated a AuGeNi electrode to form an Ohmic contact. The n^+ contact layer around the electrode was then etched away, and a second electrode (InZn) was fabricated onto the i layer, which after annealing produced an Ohmic p-type contact. In this way a horizontal p-i-n diode with a 50×50-μm gap was fabricated on top of the MQW structure to provide an in-plane electric field. The substrate was etched away under the gap to allow optical transmission. Electroabsorption measurements were performed with a 10-μm-diam probe beam to determine the field uniformly across the gap; the field appeared to be quite uniform over the entire gap region for a field of 16 kV/cm.

The laser system used was as follows. 100-fs pulses at 620 nm were synchronously amplified to 10 μJ at a 2-kHz repetition rate by using a two-stage dye amplifier pumped by a frequency-doubled Nd-doped yttrium-aluminum-garnet regenerative amplifier [6]. A white-light continuum was generated in an ethylene-glycol jet. The pump beam was selected in a 10-nm bandwidth centered at 825 nm and amplified up to 2 nJ in a single-stage

dye (LDS-821) amplifier. A 3-μm-thick GaAs thin film was used in the pump beam as a saturable absorber to prevent the ASE (amplified spontaneous emission) of the amplification stage from switching off the electric-field bias before the arrival of the pump pulse on the gap. The probe beam was passed through a four-prism chain to compensate the white-light chirp, and focused to a 20-μm spot at the center of the gap while the pump with a 50-μm diameter was overlapped with the probe. The transmission spectra of the probe were acquired on an EG&G Optical Multichannel Analyzer III. The electric field or the pump beam could be modulated to yield differential transmission spectra (DTS), with a sensitivity of 0.2% as required by the carrier densities and temperatures of our experiment. The 100-fs continuum probe pulse monitored the carrier distributions in the spectral range from -20 to $+200$ meV relative to the band edge at different delay times.

In order to observe directly the effect of the field on the carriers, DTS were taken by modulating the field, i.e., $\Delta T/T=(T_\varepsilon-T)/T$ (T_ε is the probe transmission with an electric field, and T is without a field), with the pump beam always on. Above the exciton transitions ($E>+30$ meV), the dynamic optical absorption saturation is due only to state filling by the free carriers, i.e., $\alpha(E,t)=\alpha_0(1-f_e-f_h)$, and electroabsorption has only negligible effects on α. Hence in this region $\Delta T/T\approx\Delta f_e$, i.e., the difference in the electron distribution function due to the electric field. (The contribution of the hole distribution f_h has been ignored, a simplifying assumption justified by the large heavy-hole density of states and hence smaller f.) Therefore, for example, a positive value of $\Delta T/T$ means a stronger transmission with an electric field than without a field, and thus a higher electron population.

Since heavy-hole excitons are resonantly generated in the experiment, we define $t=0$ at the maximum exciton absorption saturation with no electric field [7]. Typical DTS are shown in Fig. 1 for an applied field of nominally 16 kV/cm. The time scales of the DTS appear in three distinct regimes. (i) At energies above +30 meV, it is apparent that at early times (0 and 50 fs) there are no or small changes in the transmission, because carriers are generated at the bottom of the band. (ii) At 150 fs, a tail (from +30 meV up to +150 meV) in the DTS is clearly seen; this tail represents a positive net differential electron distribution. When the field is off, there is basically no electron population above the thermal energy of 25 meV. Thus *the appearance of electrons at energies far above the band edge is clear evidence of fast acceleration due to the applied electric field; the time scale manifests the process as ballistic acceleration.* A simple calculation (energy $=e^2\varepsilon^2t^2/2m^*$) shows that, at $\varepsilon=16$ kV/cm, a ballistic electron gains 75 meV energy from the field in 150 fs. Actually, electrons with energies above the band edge as high as 150 meV are observed; these are explained by the nonzero excitation pulse width (100 fs). Those conduction electrons that are photoinjected during the early part of the optical pulse experience the field acceleration for a time longer than 150 fs. (iii) At later times (250 and 350 fs), this high-energy tail decays, indicating an energy overshoot of the electrons confined in the QW.

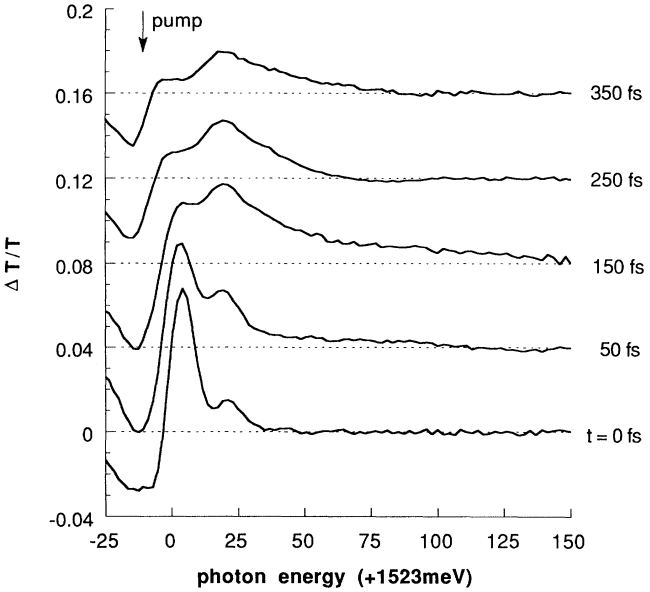

FIG. 1. Experimental differential transmission spectra, taken by modulating the electric field (between 0 and 16 kV/cm).

In order to obtain a more complete and quantitative understanding of the data, we find it more straightforward to consider the saturation of the absorption coefficient $\alpha(E,T)$, rather than the DTS directly. Hence, the field-modulated DTS and pump-modulated DTS (at zero electric field) were combined with the unmodulated absorption spectrum to reconstruct $\alpha(E,t)$, both with and without electric field.

A simple model with three components, i.e., heavy-hole exciton, light-hole exciton, and band-to-band continuum absorption, was used to fit $\alpha(E,T)$ [8]. While the electron distribution function is directly given by the absorption saturation for energies above the exciton transitions, the fitting procedure requires an assumption of the functional form of the distribution within +30 meV of the band edge. Thus we fitted the data assuming a Fermi-Dirac distribution within 30 meV of the band edge. Even with this assumption we found that it was always possible to achieve a good fit to the data, which indicates that the distribution near the band edge is always thermal, and thus carrier-carrier scattering is very strong at these densities [$(2-3)\times10^{11}$ cm^{-2}]. An example of the fitted absorption coefficient is shown in Fig. 2. We found that, with no electric field, the entire distribution was always thermal. With a 16-kV/cm field, the data could always

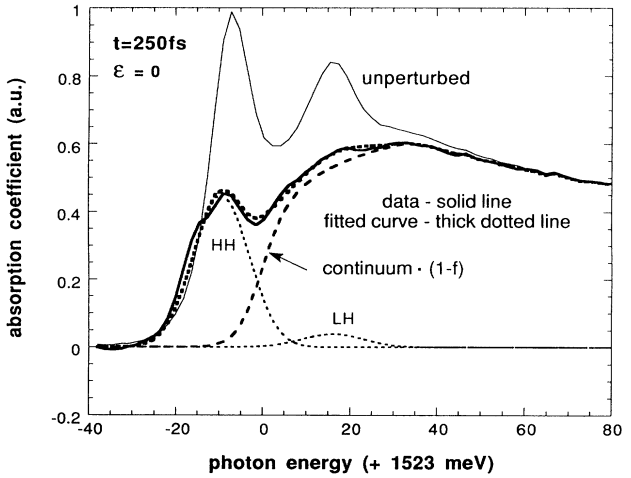

FIG. 2. A typical transient absorption spectrum $\alpha(E,t)$, shown here for the zero-field case to illustrate the fit including saturation of the heavy-hole exciton, light-hole exciton, and interband absorption. The thick solid line represents the data, the thick dotted line the fitted spectrum, and the thin dotted lines the three components. The thin solid line is the unperturbed absorption spectrum.

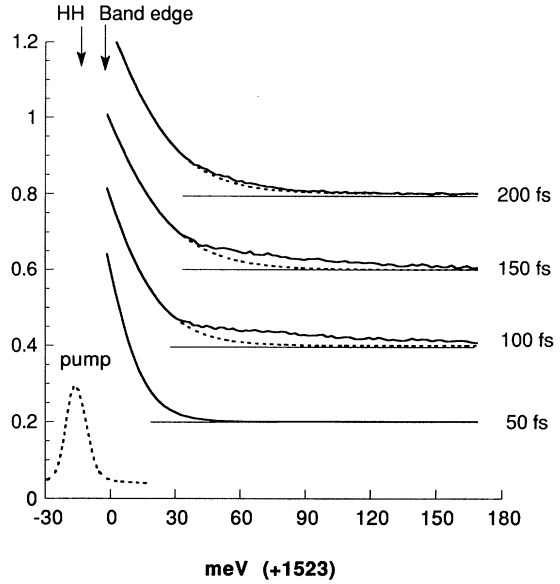

FIG. 3. Electron distribution functions obtained by fitting the transient absorption spectra for a 16-kV/cm field (solid line). The dotted line is an extension of the near-band-edge thermal distribution to higher energy. Also shown is the pump spectrum relative to the positions of the band edge and heavy-hole (HH) exciton.

be fitted with a thermal distribution near the band edge, but the transient high-energy tail discussed above was strongly nonthermal. This is apparent in Fig. 3, where we have shown representative distribution functions obtained by fitting $\alpha(E,t)$. The dotted line is an extension of the near-band-edge thermal distribution to higher energy; on the time scale of 150 fs there is clearly a nonthermal excess of electrons at high energy. After the energy overshoot (i.e., after about 300 fs), the entire distribution approaches a thermal distribution with a temperature a few meV higher than the zero-field result.

From the distribution functions, we obtained the *average* energy per electron $E_e = \int Ef(E)\,dE / \int f(E)\,dE$ in the Γ valley versus time for electric fields $\varepsilon = 0$, 8, and 16 kV/cm, as shown in Fig. 4. In the case $\varepsilon = 0$, it takes about 1.5 ps for E_e to reach room temperature. This is understood as heating of the initially cold electron-hole plasma to the lattice temperature by absorption of optical phonons [9]. The dotted line of Fig. 4 is a fit by the expression for LO-phonon scattering:

$$\frac{dT_c}{dt} = \frac{\hbar\omega_{\mathrm{LO}}}{2k\tau}\left[\frac{e^{X_L - X_C} - 1}{e^{X_L} - 1}\right]F, \qquad (1)$$

where $\hbar\omega_{\mathrm{LO}}$ is the optical-phonon energy and $X_{L,C} = \hbar\omega_{\mathrm{LO}}/kT_{L,C}$ (L denotes lattice and C carriers). The factor of 2 is for the two-dimensional system and $F \approx 0.9$ at room temperature. The best fit is obtained for a scattering time per carrier $\tau = 150$ fs. This is very consistent with other experimental results [9–11], and indicates the accuracy with which the electron distribution may be obtained using this simple fitting procedure.

With an 8-kV/cm field, the energy gain due to the relatively weak acceleration of the electrons is not much larger than the warming up solely by LO-phonon absorption.

For $\varepsilon = 16$ kV/cm, however, the average energy E_e

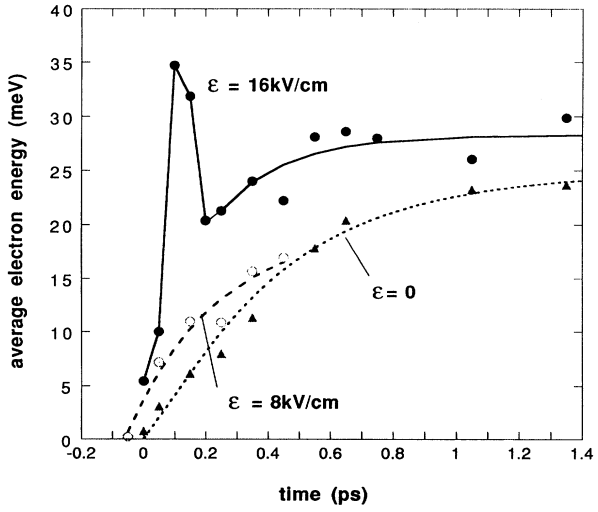

FIG. 4. Average energy per electron obtained from the fitted distribution functions for three different electric fields. For the zero-field case, the dotted line is a fit to the data using Eq. (1) in the text. For $\varepsilon = 8$ and 16 kV/cm, the dashed and solid lines are simply guides to the eye.

shows a rapid rise to about 35 meV in 100 fs, which corresponds to the growth of the nonthermal high-energy electrons. The average energy then exhibits an overshoot, and reaches a steady-state value only 5 meV above room temperature. Though the rapid energy increase is understood as a ballistic effect, the details of the factors that cause the energy overshoot are not yet clear. One factor contributing to the overshoot is that the electric field in the gap relaxes rapidly for the high carrier densities used in this experiment, as indicated by the low final average energy. The field relaxes as the electrons and holes accelerate, producing a space charge which acts to oppose the applied field. In fact, the fast buildup of this space-charge dipole results in the generation of electromagnetic radiation (a well-known phenomenon of photoconductive switches [12]), which acts to rapidly reduce the total field in the gap. Finally, the maximum energy of the electrons is limited by the fact that, since the electromagnetic energy stored in the gap region cannot be replenished by the external bias supply on the time scale of the transients discussed here, the total field will relax as the electrons gain energy from the field.

A second contribution to the overshoot is that electrons that have been accelerated to sufficiently high energy can scatter into the continuum states above the barrier (i.e., the so-called real-space transfer [13]) or at higher energies undergo intervalley scattering, where they no longer contribute to E_e, the energy per carrier in the well. Further investigations are in progress to determine the relative contribution of the field relaxation and the real-space transfer. Experimentally, it is required to reduce the carrier density injected into the wells in order to reduce the switching off of the applied field. On the theoretical side, it is required to model the transport of the electrons in the gap region in a self-consistent way [14]. That is, not only must the acceleration and scattering of the carriers be modeled, but the response of the electrons to the *total* electric field in the gap, i.e., the space-charge field plus the transient field generated by the accelerating electrons, must be considered.

In conclusion, we have applied femtosecond time-resolved spectroscopy to study the ballistic acceleration of electrons in a GaAs quantum-well structure. In contrast to the well-studied relaxation processes in GaAs, this is a novel experiment which investigates the reverse process, i.e., heating of the carriers by an external electric field. We have shown that for a 16-kV/cm electric field ballistic acceleration can be observed on a time scale of about 150 fs.

We would like to thank Bob Grondin, Gerard Mourou, and June-Koo Rhee for useful discussions. This work was supported by the AFOSR under Grant No. URI-090-0214.

---

[a]Also with the Applied Physics Department.

[1] A. F. Levi, J. R. Hayes, P. M. Platzman, and W. Wiegmann, Phys. Rev. Lett. **55**, 2071 (1985).

[2] M. Heiblum, M. I. Nathan, D. C. Thomas, and C. M. Knoedler, Phys. Rev. Lett. **55**, 2200 (1985).

[3] U. Sivan, M. Heiblum, and C. P. Umbach, Phys. Rev. Lett. **63**, 992 (1989).

[4] J. L. Oudar, D. Hulin, A. Migus, A. Antonetti, and F. Alexandre, Phys. Rev. Lett. **55**, 2074 (1985).

[5] J. Shah, IEEE J. Quantum Electron. **22**, 1728 (1986), and references therein.

[6] I. N. Duling, T. Norris, T. Sizer, P. Bado, and G. A. Mourou, J. Opt. Soc. Am. B **2**, 616 (1985).

[7] W. H. Knox, R. L. Fork, M. C. Downer, D. A. B. Miller, D. S. Chemla, C. V. Shank, A. C. Gossard, and W. Wiegmann, Phys. Rev. Lett. **54**, 1306 (1985).

[8] D. S. Chemla, D. A. B. Miller, P. Smith, A. Gossard, and W. Wiegmann, IEEE J. Quantum Electron. **20**, 265 (1984).

[9] W. W. Rühle and H.-J. Polland, Phys. Rev. B **36**, 1683 (1987).

[10] J. A. Kash, J. C. Tsang, and J. M. Hvam, Phys. Rev. Lett. **54**, 2151 (1985).

[11] M. Heiblum, D. Galbi, and M. Weckwerth, Phys. Rev. Lett. **62**, 1057 (1989).

[12] D. H. Auston, K. P. Cheung, and P. R. Smith, Appl. Phys. Lett. **45**, 284 (1984).

[13] K. Hess, H. Morkoc, H. Shichijo, and B. G. Streetman, Appl. Phys. Lett. **35**, 469 (1979).

[14] S. El-Ghazaly, P. R. Joshi, and R. O. Grondin, IEEE Trans. Microwave Theory Tech. **38**, 629 (1990).